# Tectonic control on River bed Incision

*"The most beautiful experience we can have is the mysterious. It is the fundamental emotion that stands at the cradle of true art and true science."*

**— Albert Einstein, the World As I See It**

**Dr. N.L. Dongre**

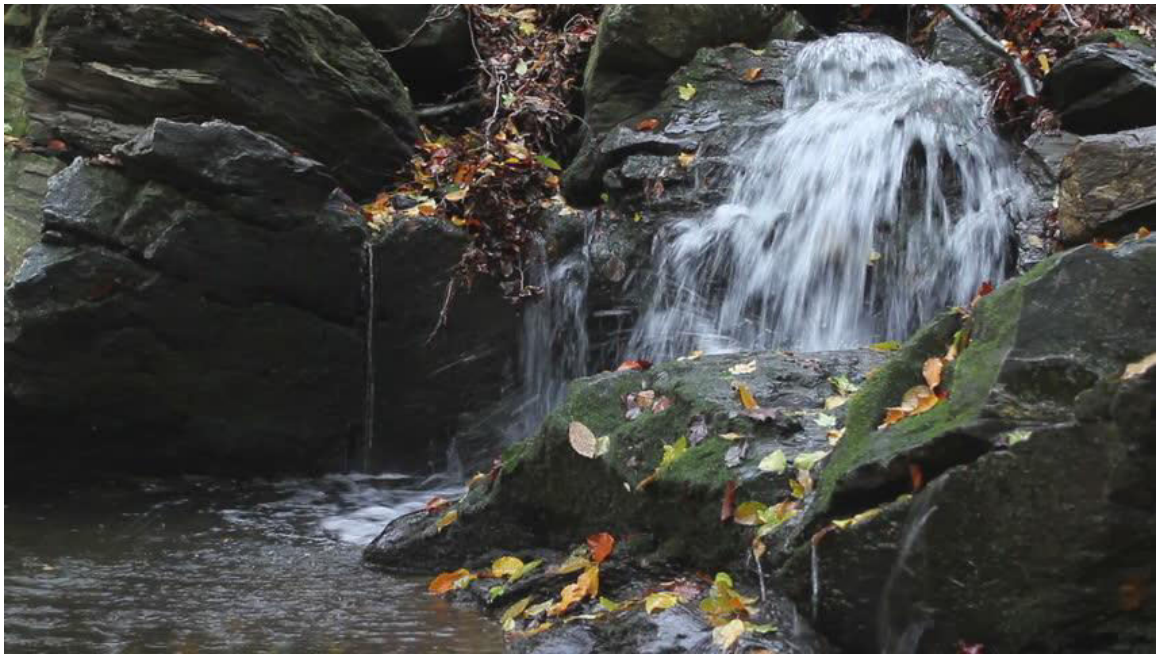

The waterfall on Gudra River of Abujhmarh, India. The response of bedrock channel to footwall uplift events leads to the faulting activities related to perturbations and displacement.

---


## Abstract

**[1] Here we investigated that the evolution of footwall drainage basins, sediment supply and hanging wall stratigraphy in rift basins. We presented a coupled numerical model of detachment-limited stream network evolution and coarse-grained fan delta deposition. The result of bedrock channel networks to repeated footwall uplift events leads to increasing sediment supply over tens of thousands of years as the networks initiate and then expand, followed by relatively constant sediment supply as the stream networks reach their maximum spatial extent. The distinct time lag between the onset of tectonic activity and attainment of maximum sediment supply leads to stratigraphies that are initially a gradational and then progradational. Much of the variation in sediment supply is the product of the complex response and reorganization of the stream networks to faulting-related perturbations and is not directly related to specific faulting events. Increasing fault displacement drives the system toward a new steady state with a higher sediment supply but is initially expressed as a retro gradation as sediment supply lags behind increased**

**displacement. The converse is true for a decrease in fault displacement, which is initially expressed as progradation. Continual stochastic variation in recurrence interval leads to a system that does not achieve a steady state and as a result exhibits continual variation in sediment supply. The model results emphasize the local tectonic controls on stratigraphic architectures developed within extensional basins and the complex manner in which stream network growth and response to tectonic activity can be expressed in the stratigraphic record.**

---

## 1. Introduction

[2] The landscape topographic evolution of many tectonically active regions is arguably dominated by the rates and patterns of bedrock channel incision [*Stock and Montgomery*, 1999; *Snyder et al.*, 2000; *Whipple et al.*, 2000a, 2000b]. Bedrock channels are a major component of mountainous drainage basins and it appears that in tectonically active mountain ranges the elevation drop on bedrock channels comprises 80–90% of drainage basin relief [*Whipple et al.*, 1999]. The initiation, organization, and evolution of such bedrock channel networks, and their response to tectonic activity and climate change, are thought to have a profound, first-order, effect upon sediment supply to basins. In particular, mountainous catchments dominated by bedrock channels are often the sediment source for coarse-grained deltas, the focus of much recent (sequence) stratigraphic research as they have the potential for recording tectonic, climatic, and eustatic variations in their preserved stratigraphy [e.g., *Colella*, 1988; *Gawthorpe and Colella*, 1990; *Dart et al.*, 1994; *Dorsey et al.*, 1995, 1997; *Young et al.*, 2000]. However, despite the first-order control of sediment supply on stratigraphic architecture, our knowledge of both the magnitude and frequency of variations in sediment supply to basins is limited. A better understanding of drainage basin response to changing tectonic and climatic boundary conditions is therefore of fundamental importance if the stratigraphic architectures preserved in ancient basins are to be used to assess changes in tectonic activity, eustatic sea level and climate over geological timescales. In an effort to address this issue, we have developed a numerical model to investigate the development of bedrock channel dominated drainage basins in the footwalls of extensional fault blocks, their effect on sediment supply to hanging wall basins, and the implications for the interpretation of stratigraphic architectures developed in coarse-grained deltas.

[3] In recent years much research has been undertaken into the processes controlling stream network development and, more generally, landscape evolution, leading to the development and testing of a variety of stream network and landscape evolution models (LEMs) [e.g., *Stark*, 1991; *Rigon et al.*, 1994; *Howard*, 1994; *Tucker and Slingerland*, 1996, 1997; *Rinaldo et al.*, 1995; *Caldarelli et al.*, 1997; *Rodriguez-Iturbe and Rinaldo*, 1997; *Densmore et al.*, 1998; *Van der Beek and Braun*, 1999; *Pelletier*, 1999; *Stock and Montgomery*, 1999; *Whipple and Tucker*, 1999; *Snyder et al.*, 2000; *Veneziano and Niemann*, 2000a, 2000b]. However, while these studies have provided a better understanding of the major controls on drainage basin morphology and evolution, the relationship between stream network/landscape evolution and sediment supply to adjacent sedimentary basins has received only limited study [e.g., *Howard*, 1994; *Tucker and Slingerland*, 1996, 1997; *Densmore et al.*, 1998]. In addition, the stratigraphic signature (in basinal sediments) of drainage basin growth, and response to climatic or tectonic forcing, has not been investigated. In parallel with these studies, numerical models of tectonics and sedimentation in two and three dimensions applicable to clastic deposition have been developed and have furthered our understanding of the controls on the preserved stratigraphies in extensional basins and other settings [e.g., *Hardy et al.*,

1994; *Hardy and Gawthorpe*, 1998; *Driscoll and Karner*, 1999; *Ritchie et al.*, 1999]. However, these models have treated sediment supply as constant or a known input to the particular numerical model, rather than considering drainage basin evolution and sediment deposition as a coupled system. Thus there is no inherent temporal or spatial variability in sediment supply in these models other than that imposed as part of an experiment, and no link between the evolving drainage basin and the depositional realm.

[4] This paper aims to build on this research by developing a numerical model of linked stream network (bedrock channel) evolution and coarse-grained clastic deposition associated with extensional faulting. It is not our intention to propose or develop another LEM but rather to use an existing LEM to drive a model of coarse-grained clastic deposition. The coupled model is based on the well-known stream power (or similar shear stress) erosion law for stream network/landscape evolution [see, e.g., *Whipple and Tucker*, 1999] and a random walk/diffusion algorithm for coarse-grained clastic deposition [*Hardy and Gawthorpe*, 1998]. Stream network evolution is modeled using a critical threshold stream power erosion law for fluvial incision applicable to the development of bedrock channels. Such threshold stream power/shear stress models have been shown to capture the fundamental structure and behavior of many river networks [e.g., *Rigon et al.*, 1994; *Rodriguez-Iturbe and Rinaldo*, 1997; *Talling*, 2000]. We do not include hillslope diffusive transport or landsliding in our landscape evolution model. The model of coarse-grained clastic (fan delta) deposition uses a random walk algorithm for three-dimensional (3-D) sediment delivery from the drainage basin outlets to the shoreline, together with a nonlinear (threshold) 3-D diffusion equation for sediment movement on steep delta foresets. The model of clastic deposition has previously been shown to reproduce the morphologies of, and stratigraphic architectures within, small, coarse-grained deltas [*Hardy and Gawthorpe*, 1998; *Ritchie et al.*, 1999]. We feel that the coupled model encapsulates many of the essential elements of the system and may allow a better understanding of the inherent spatial and temporal variability of sediment supply in such settings and its expression in the stratigraphic record. The implications of the model results for the use of deltaic stratigraphies as proxies for climatic or tectonic signals in the geological record are discussed.

## 2. Methodology

[5] We use a simple lattice or cellular, forward model of coupled stream network (drainage basin) evolution and fan delta deposition. The lattice model is square with dimensions of 200 × 200 representing an area of 10 km by 10 km and is divided into two parts separated by an extensional fault. The hanging wall of the fault undergoes subsidence while the footwall undergoes uplift producing marine and terrestrial areas respectively. Displacement on the fault is simplified to include only vertical motion and thus neglects the horizontal component of displacement [cf. *Hardy et al.*, 1994; *Hardy and Gawthorpe*, 1998]. The drainage basin evolution model is applied to the uplifting, terrestrial region in the footwall of the fault, while the model of fan delta deposition is operative in the hanging wall (marine) portion of the model (see Figure 1a). The two algorithms are detailed in the following sections.

### 2.1. Drainage Basin Evolution Model

[6] The model of drainage basin evolution used here is based upon a stream power (or similar shear stress) erosion law and is a simple model of one important aspect of landform evolution: the fluvial dynamics of bedrock channels. Our choice of this LEM is based on its simplicity, which enables us to isolate the effects of the fluvial dynamics of bedrock channels on sediment supply to sedimentary basins. The evolution of the fluvial network is based upon a dynamic threshold for fluvial activity (erosion) defined by the exceedance of a critical threshold.

While the dynamics are extremely simple, approaches of this type have been shown to reproduce the recurrent scale-free landforms typical of river basins, with scaling behavior in agreement with that of natural river basins [*Rigon et al.*, 1994; *Caldarelli et al.*, 1997; *Rodriguez-Iturbe and Rinaldo*, 1997].

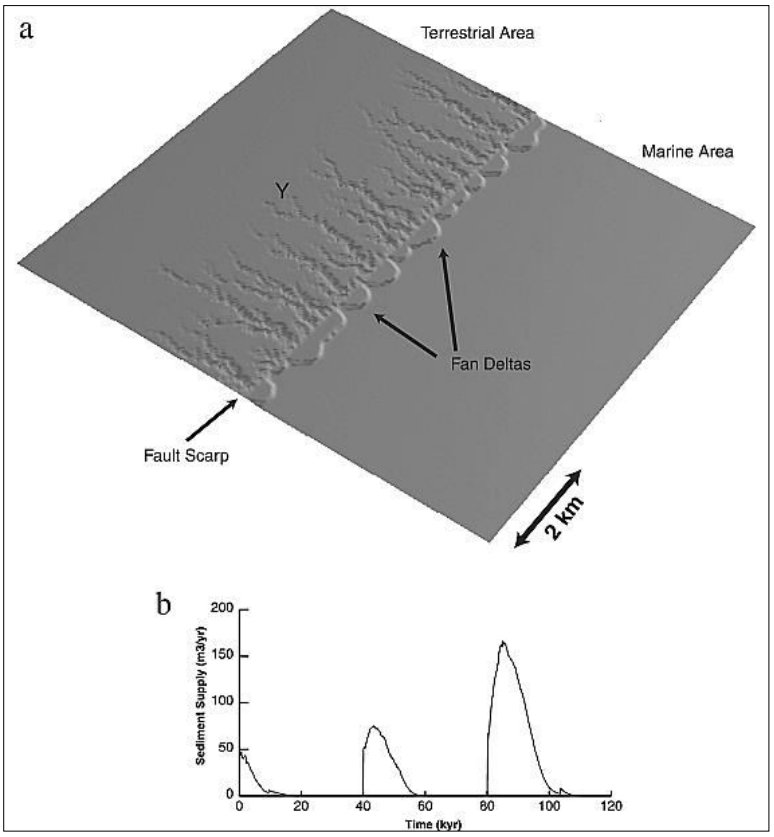


Figure 1. (a) Surface morphology of coupled stream network clastic deposition model 120,000 years after three instantaneous footwall uplift events. The value of the critical threshold for erosion used is 5.0 $m^{0.8}$. Vertical exaggeration is 2. (b) Sediment supply versus time delivered from the catchment labeled Y indicated in the model shown in Figure 1a.

[7] The drainage basin model is defined as follows: all of the lowest terrestrial sites of the lattice are considered to be possible outlets of a suite of rivers, which are competing to drain the terrestrial area. A steepest descent algorithm is used to assign a drainage direction from each of the cells to one of its eight nearest neighbors. Each cell collects water from a distributed injection (rainfall), in addition to the flow that drains to that cell from upstream, connected cells. The drained area (used empirically a measure of the total flow) of each site $x$ is calculated over all sites whose area is drained by $x$. If no contribution to $x$exists, then it is a source cell. Fluvial incision and stream network development are modeled as follows: the stream power, $P$, acting on every site is computed as

$$P_x \propto A^m S^m, \tag{1}$$

where $A$, the total upstream contributing area, is used as a proxy for discharge at that site and $S$ is the local gradient along the drainage direction (see *Caldarelli et al.* [1997], *Rodriguez-Iturbe and Rinaldo*[1997], *Whipple and Turner* [1999], and *Talling* [2000] for a more complete discussion on this approach). As such, $Px$ depends on both local conditions (the local gradient) and on nonlocal conditions defined by the contributing area at that location. The exponents $m$ and $n$ are positive constants that depend on erosion process, basin hydrology, and

channel geometry [see, e.g., *Whipple et al.*, 2000b]. The ratio of *m*/*n* is theoretically predicted to lie in a narrow range around 0.5 ($0.35 \leq m/n \leq 0.6$) [*Whipple and Tucker*, 1999]. The values of *m* (0.4) and *n* (1.0) used in the modeling presented here are chosen in order that direct comparison can be made with recent calibrations of the stream power incision law reported in the literature [*Stock and Montgomery*, 1999; *Whipple et al.*, 2000a].

[8] If the calculated stream power on a site exceeds a threshold value, $P_{\text{crit}}$, then fluvial incision occurs, with the incision rate given by a linear function of the stream power in excess of the critical threshold [cf. *Howard*, 1994; *Tucker and Slingerland*, 1997]:

$$\frac{\partial h}{\partial t} = -K[P_x - P_{\text{crit}}], \tag{2}$$

where *h* is the height (m) of a cell, *t* is time (years), and *K* is a dimensional coefficient of erosion [see *Stock and Montgomery*, 1999; *Whipple and Turner*, 1999; *Snyder et al.*, 2000; *Whipple et al.*, 2000a]. The critical threshold can be thought of as a lower limit for channel initiation (controlling the location of channel heads) and describes the land surface resistance to erosion by surface flow [*Tucker and Slingerland*, 1997]. It thus sets the bounds on the drainage density in the model (the balance between hillslopes and channels); we have investigated the response of the model to a range of values of the critical threshold. The value of the coefficient of erosion *K* is, as yet, not well calibrated, but recent work has suggested it can vary by several orders of magnitude and that it lies in the range $10^{-3}$ to $10^{-7}$, the units of *K* ($\text{m}^{1-2m}\ \text{yr}^{-1}$) depending upon the exponents of the contributing area and slope in equation (1). The value of *K* probably depends on a variety of factors such as discharge, rock strength, channel width, and sediment load [e.g., *Stock and Montgomery*, 1999; *Whipple and Tucker*, 1999; *Snyder et al.*, 2000].

[9] As the drainage basin model is coupled to our depositional model, at each time step the sediment volume eroded by the evolving stream network(s) is calculated and routed to the drainage basin outlets which are located along the extensional fault scarp (Figure 1a). As we are interested in modeling bedrock channels, we assume that all streams have the capacity to entrain and transport particles in excess of the local sediment supply; that is, all eroded material is transported out of the system without redeposition within the drainage basin (a detachment-limited system). Thus the sediment supply ($\text{m}^3\ \text{yr}^{-1}$) is calculated through space and time at these locations and is then transported to, and deposited within, the marine hanging wall basin (Figure 1a). In the simulations described below we assume that all of the material eroded by fluvial activity is converted into coarse-grained bed load, and thus we do not take account of dissolution of carbonates, suspended load, etc., and their effect on depositional architectures.

### 2.2. Coarse-Grained Clastic Deposition Model

[10] Within the coupled model, coarse-grained clastic (deltaic) deposition is modeled by applying the algorithm of *Hardy and Gawthorpe* [1998] at each time step. The sediment supply ($\text{m}^3\ \text{yr}^{-1}$) calculated from the drainage basin evolution model is delivered to each drainage basin outlet (point source) at the hanging wall-footwall junction (the extensional fault scarp). From this location a decision is made (using a random walk algorithm) to go to a neighboring cell, and this process is repeated until the shoreline is reached, i.e., at the first cell encountered that is below sea level. This random walk is constrained such that it cannot go backward into the drainage basin (footwall). When the shoreline is encountered by a random walker, the sediment supply is deposited in that cell, thereby increasing its height and, if all accommodation space is filled, leading to local progradation of the shoreline. If the sediment supply is greater than accommodation at this cell, the process is repeated in adjacent "wet" cells. This progradation

ensures that the shoreline at this site is further away from the source cell, and thus a closer shoreline cell is more likely to be encountered by a random walker at the next time step. Overall, this leads to radial progradation of the delta over periods of thousands of years but localized progradation over periods of tens to hundreds of years. Further details of the algorithm are given by *Hardy and Gawthorpe* [1998] and *Ritchie et al.* [1999]. We feel that this algorithm captures much of the complexity of the delivery of sediment from source to shoreline and the radial nature of fan delta progradation. Slopes between all cells are monitored, and if they are greater than a critical angle, slope failure is simulated by using a discrete threshold (nonlinear) diffusion algorithm [cf. *Bak et al.*, 1988]. A diffusion model assumes that sediment flux is proportional to local slope and in the down slope direction. This assumption results in redistribution of material from a locally over steepened cell to its down slope neighbors, simulating slumping and other slope processes.

## 3. Experimental Results

[11] The initial surface used in the model experiments is gently tilted seaward at ~0.5° and, in order to have unbiased initial conditions, has random, uncorrelated noise of up to 0.50 m added to the surface height. The model is square with dimensions of 200 × 200 representing an area of 10 km by 10 km. The cell size and time step used in the simulations are 50 m and 100 years, respectively. In the terrestrial part of the model we use a value of $K$, the coefficient of erosion in the stream power erosion law, of $5 \times 10^{-4}$ $m^{0.2}yr^{-1}$. This value is chosen as it lies within the wide range of previously published estimates of $K$ [cf. *Stock and Montgomery*, 1999; *Whipple et al.*, 2000a; *Snyder et al.*, 2000]. The exponents $m$ (0.4) and $n$ (1.0) used in the stream power erosion law are chosen in order that direct comparison can be made with recent calibrations reported in the literature [*Stock and Montgomery*, 1999; *Whipple et al.*, 2000a]. A range of values of the critical threshold ($P_{crit}$) have been tested, and while the specific results are different, the basic conclusions drawn are the same as those presented in the model below where we use a value of 5.0 $m^{0.8}$. In the marine part of the model a critical slope angle of 30° is used for the foreset angle of repose of the coarse-grained sediments [cf. *Nemec*, 1990]; for steeper angles, slope processes (diffusion) become active through using a diffusion coefficient of 3.0 $m^2$ $yr^{-1}$, and for shallower angles the diffusion coefficient is zero, and slopes are considered to be stable [cf. *Hardy et al.*, 1994].

[12] Described below are three experiments showing the response of the model to (1) single, isolated faulting events, and (2) repeated faulting events over geological timescales. The results presented below are representative of many realizations of the model under the specified boundary and initial conditions.

### 3.1. Response to Single, Isolated Faulting Events (Instantaneous Uplift and Subsidence)

[13] The effect of instantaneous faulting events which cause 5 m of uplift in the footwall of the extensional fault, and a corresponding subsidence of 5 m in the hanging wall, on the organization of the stream networks and the evolution of sediment supply is considered in this section. While these values are unrealistic for an individual (coseismic) faulting event, they allow us to investigate the basic behavior of the model and the effect of an uplift event on stream network development and sediment supply. The response of the model will be assessed by modeling three distinct uplift events: one at the start of the model run to initiate a stream network, a second after 40,000 years, and the final after 80,000 years. The model is run for a total of 120,000 years.

[14] The final surface morphology of the model is shown in Figure 1a; at this stage the model has reached equilibrium and all links in the drainage networks are at, or below, the critical threshold required to initiate erosion. The drainage networks developed can be seen to be small, extending 500–2500 m into the footwall from the fault and to have a dominantly parallel to dendritic form. The stream networks in the model initiated at the fault "scarp" and have grown head wardly, perpendicular to the fault, by approximately equal amounts, leaving much of the footwall topography unaffected by fluvial erosion. Concurrent with this headward growth, the networks also grew by the addition of tributaries to the initial low-order streams. In the hanging wall basin, small deltas have formed at the outlets of the drainage basins, although over the time period of 120,000 years the volume of sediment delivered to the marine basin is small compared to the accommodation space created. Note that the deltas are essentially isolated along strike, although two or three channel networks feed the larger deltas. Model experiments using lower values of the critical threshold lead to more extensive stream networks as an increasing proportion of the footwall is affected by fluvial erosion and becomes channelized, while those using higher values produce more spatially restricted networks leaving much of the footwall unaffected by erosion.

[15] The sediment supply delivered to the marine basin from a representative stream network (labeled Y in Figure 1a) through time is shown in Figure 1b. It can be seen that after the first uplift event there is a pulse of sediment supply as the stream network is initiated and a wave of incision migrates into the footwall. After peaking at ~50 $m^3\ yr^{-1}$ the sediment supply decays exponentially as the stream network reaches its maximum spatial extent and the system approaches equilibrium, when all cells in the model are at, or below, the critical threshold for fluvial erosion. Twenty thousand years after the first uplift event the sediment supply has fallen to zero and the system is in equilibrium. The second and third uplift events, at 40 and 80 kyr, respectively, cause an immediate, abrupt increase in sediment supply as the stream network is no longer in equilibrium and a wave of erosion propagates from the fault scarp into the footwall. This causes further headward and lateral growth of the stream network. The sediment supply reaches a maximum ~5 kyr after each uplift event, where after it decays rapidly and the system reattains equilibrium within ~20 kyr. Peak sediment supply after the second event is ~75 $m^3\ yr^{-1}$, while after the third event it increases to ~170 $m^3\ yr^{-1}$. This increase in peak sediment supply is a result of the growth (expansion) of the stream network in response to repeated uplift events leading to an increasing total stream length with time. This results in many more potential sites for erosion as uplift-related base level perturbations propagate through the system. With further events the stream network would eventually reach its maximum spatial extent and reach a steady state producing a constant sediment supply in response to uplift events.

[16] The above model has shown the initiation and response of footwall stream networks to single "earthquake" uplift events. The streams networks are allowed to develop and reach equilibrium without being reperturbed by further uplift events. Thus the recurrence time of the uplift events is much greater than the response time of the system. In contrast, the models described below will investigate geologically more realistic scenarios where repeated faulting events occur and affect preexisting footwall topography with established and/or evolving stream networks. These stream networks may still be responding to a previous uplift event when they are affected by a subsequent event.

### 3.2. Response to Repeated Faulting Events over Geological Timescales

#### 3.2.1. Constant Recurrence Interval

[17] The second experiment will show the response of the model to repeated faulting events over a longer timescale of 600,000 years. This model is intended to address the variability

of sediment supply over geological timescales which might potentially be recognized/recorded in deposits from ancient rift systems. We introduce faulting as discrete uplift/subsidence events occurring at a constant recurrence interval of 1000 years. These events cause the hanging wall to subside by 1.0 m and the footwall to uplift by 0.5 m, values which are broadly within the range of values reported from the literature [see *Hardy et al.*, 1994; *Gawthorpe et al.*, 1994; *Leeder*, 1991]. All other model parameters are identical to those used in the previous model.

[18] The evolution of the model is shown in Figure 2. As before, it can be seen that the stream networks initiate at the fault scarp and then develop by headward growth into the footwall in a direction approximately normal to the fault scarp. Rates of fluvial incision produced by the model are in the range 0–100 cm $kyr^{-1}$ consistent with reported bedrock channel incision rates from Recent and Quaternary drainage basins [*Tinkler and Wohl*, 1998]. In the hanging wall a series of initially discrete deltas is produced at the outlets of the evolving drainage basins (Figures 2a–2c). As uplift continues and the stream networks continue to grow, the deltas coalesce to form an almost continuous fringe or bajada up to 2 km in width along the fault trace (Figures 2d–2f). The final footwall landscape developed consists of a series of small (typically 5.0–8 $km^2$), narrow, steep drainage basins trending normal to, and spaced at approximately equal intervals (~1 km) along, the fault trace (Figure 3a). Many typical morphologic features such as ridges, spurs, and truncated (faceted) spurs are present in the final footwall topography which is flanked by a bajada-like apron of deltaic deposits. From a qualitative morphologic standpoint the final landscape appears realistic and is comparable to the footwalls of active normal faults such as those seen in the Basin and Range [*Leeder and Jackson*, 1993] and the Aegean [*Goldsworthy and Jackson*, 2000]. The longitudinal stream profiles produced are smooth and concave upwards becoming steep in their headwaters (Figure 3b), similar to those reported from drainage basins in tectonically active settings [e.g., *Snyder et al.*, 2000]. Slopes in the upper reaches are typically 0.1–0.2, while the lower reaches are essentially linear with slopes of ~0.01.

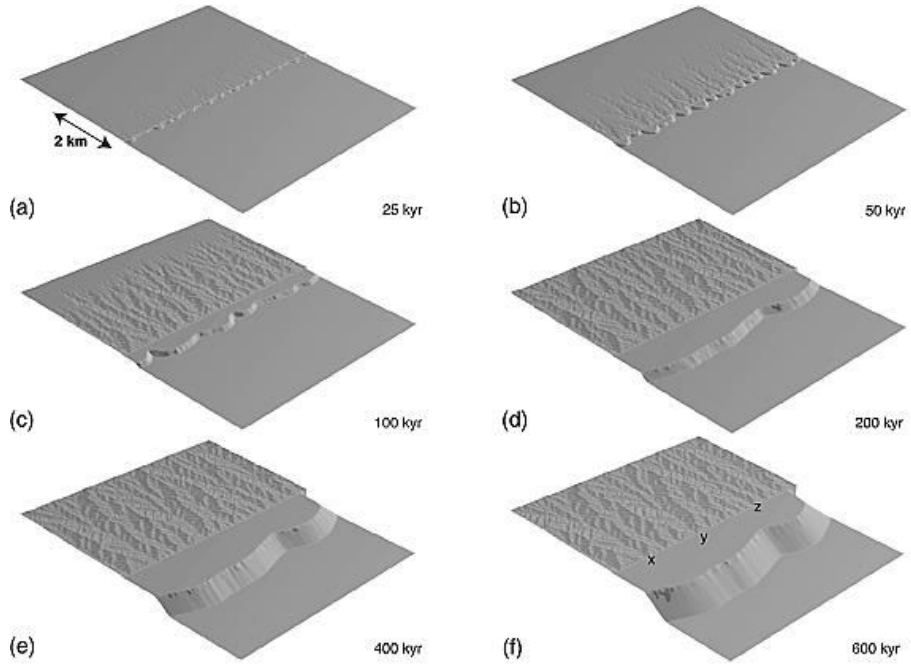


Figure 2. Progressive development of a model with repeated earthquake events producing 0.5 m of uplift and 1.0 m of subsidence every 1000 years over a total run time of 600,000 years. The value of the critical threshold for erosion used is 5.0 $m^{0.8}$. All other model parameters as in Figure 1. No vertical exaggeration.

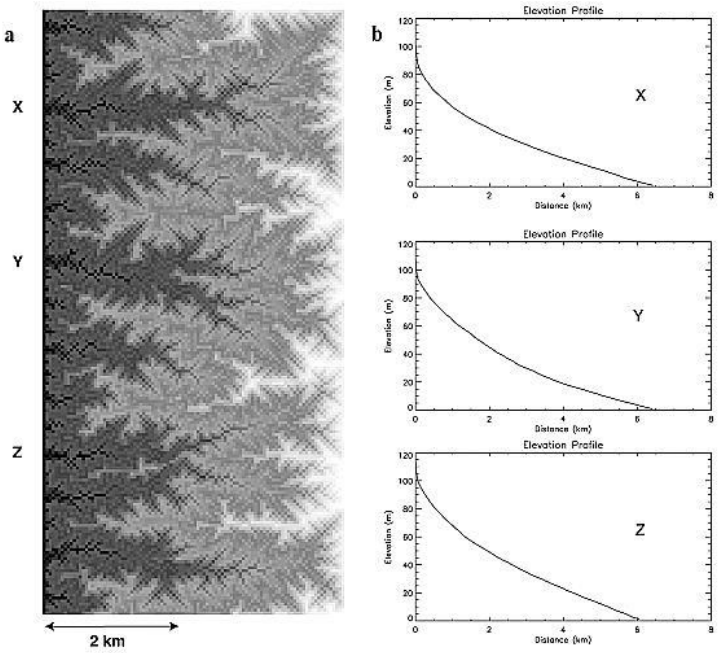


Figure 3. (a) Map view of footwall drainage basins at end of model run shown in Figure 2f. (b) Representative stream profiles for three catchments (labeled X, Y, and Z) developed on the landscape.

[19] We have performed river network extraction and analyses on the final landscape of Figure 2 using the software River Tools 2.0. Natural landscapes show several power law relationships between the morphologic components of river basins, in particular those based on the Strahler stream-ordering scheme. Figure 4 shows the relationships between some significant geomorphic components of the final landscape: for a given Strahler order, the average number of streams $N$ as a function of the average drainage area $A$ (Figure 4a), the average along channel slope $S$ as a function of the average drainage area $A$ (Figure 4b), the average main channel length $L$ as a function of the average drainage area $A$ (Figure 4c), the average basin relief $R$ as a function of the average drainage area $A$ (Figure 4d), the cumulative probability of contributing area $P[A \geq a]$ for all channel links (Figure 4e), and the cumulative probability of main channel length $P[L \geq l]$ for all channel links (Figure 4f). From Figures 4a–4f it can be seem that all the relationships between variables show very good power law relationships given by

$$N \propto A^{p}$$

$$L \propto A^{q}$$

$$S \propto A^{r}$$

$$R \propto A^{s}$$

$$P[A \geq a] \propto a^{\beta}$$

$$P[L \geq l] \propto l^{\gamma}$$

The values of the scaling exponents $p$ (−1.043), $q$ (0.583), $r$ (−0.389), and $s$ (0.218) derived from the final model landscape are in good agreement with those reported from real river basins [see *Pelletier*, 1999]. Despite finite-size effects being visible, the probability distributions

of contributing area and main channel length (Figures 4e and 4f) can also be seen to obey clear power law relationships that are an indicator of the fractal structure of the stream network [see *Rodriguez-Iturbe and Rinaldo*, 1997]. The values of the scaling exponents β and γ for the power laws (−0.41 and −0.80) are similar to those reported from theoretical modeling studies and to those found in real river basins [*Rodriguez-Iturbe and Rinaldo*, 1997]. Given the match between our model river networks and the observed scaling laws of real river networks, we are confident that the model produces morphologically realistic landscapes over geological timescales.

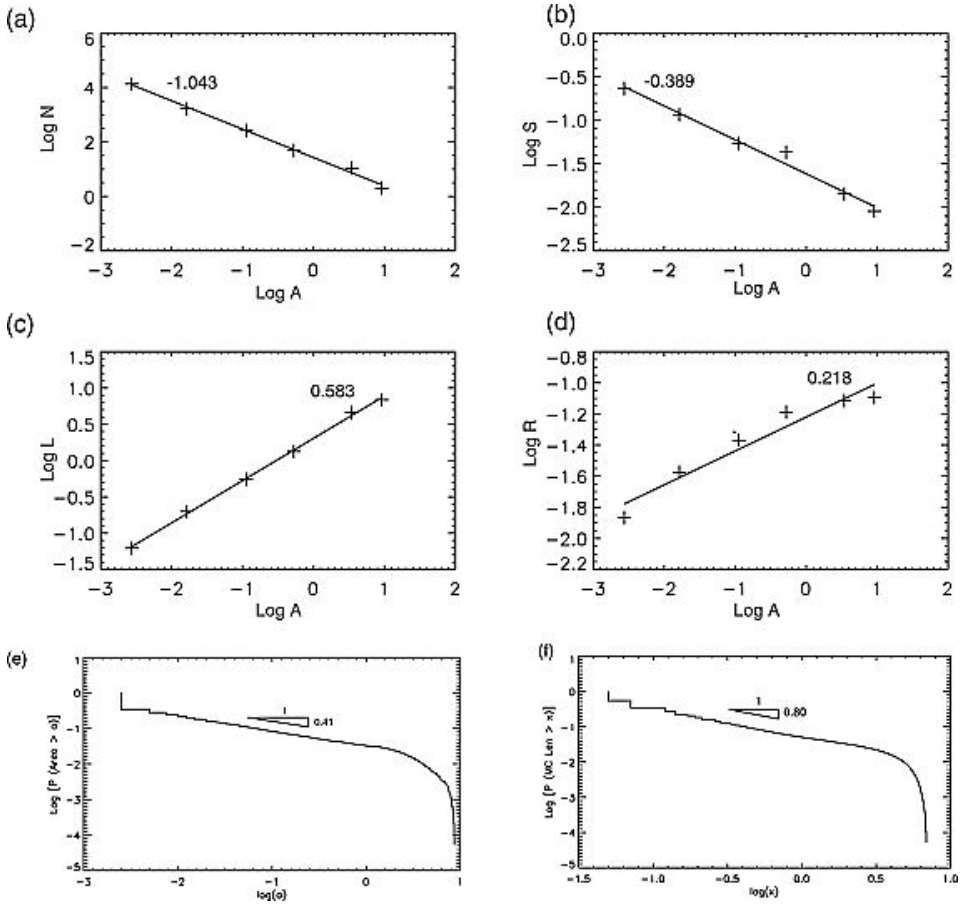


Figure 4. For the landscape shown in Figure 2f plots of, for a given Strahler order, (a) the average number of streams *N* as a function of the average drainage area *A*, (b) the average main channel length *L* as a function of the average drainage area *A*, (c) the average basin relief *R* as a function of the average drainage area *A*, (d) the average along channel slope *S* as a function of the average drainage area *A*, (e) cumulative probability of contributing area for all channel links, and (f) cumulative probability of main channel length for all channel links.

[20] The evolution of sediment supply delivered from three representative stream networks (labeled X, Y, and Z in Figure 2) in the model is shown in Figure 5. In each case it can be seen that the sediment supply progressively increases up to ~125–150 kyr. This is followed by a period of ~250 kyr during which sediment supply is relatively constant but still displays significant variation. The detailed response of stream network Y during the period 250–350 kyr is shown in Figure 6. It can be seen that a signal from the tectonic forcing (uplift) is discernible as small pulses in sediment supply with a frequency of 1 kyr. However, during much of the time interval the sediment supply shows much greater variation (~200 $m^3 yr^{-1}$) with two peaks at ~275 and ~310 kyr which have no obvious or direct relationship to specific faulting events. The

system moves toward a steady state after ~400 kyr where only minor further topologic adjustments are possible and the network configuration is essentially frozen resulting in approximately constant sediment supply from all three catchments (Figure 5).

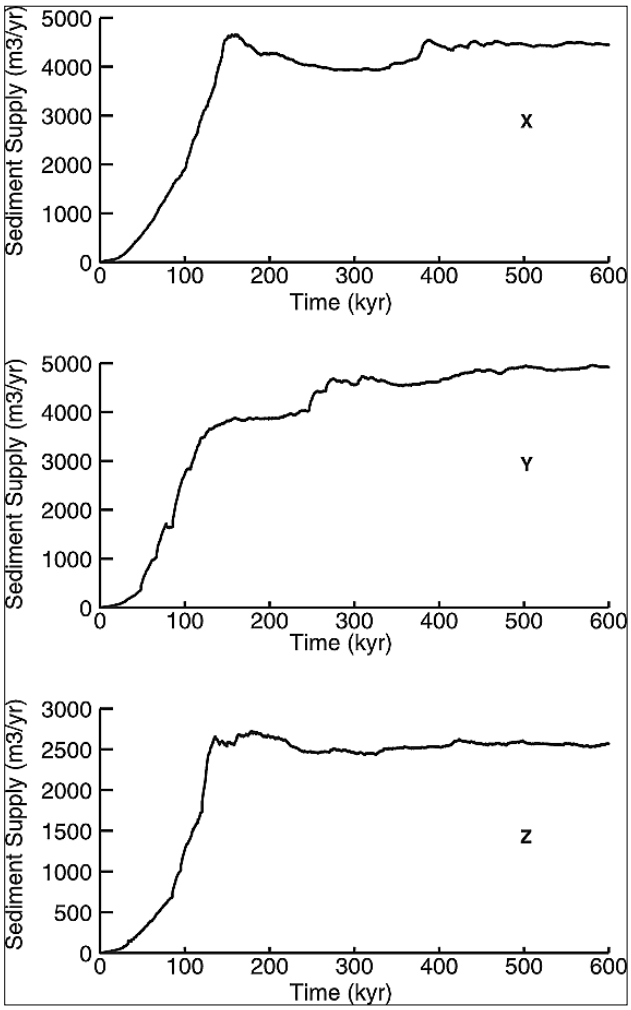


Figure 5. Sediment supply versus time for the catchments X, Y, and Z indicated in the model shown in Figure 2.

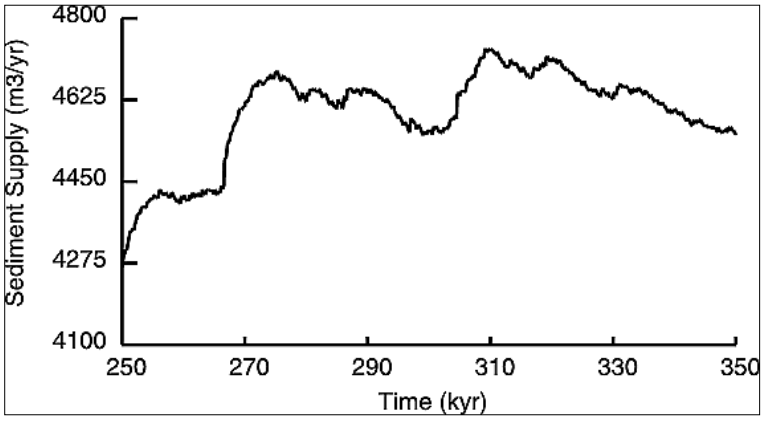


Figure 6. Detail of sediment supply variations with time for catchment Y over the period 250 to 350 kyr.

[21] We have investigated the effect of a range of values of the critical threshold for erosion on the development of the drainage networks and sediment supply in our model. Figure 7 shows sediment supplies from catchment X under a range of different critical thresholds (2.5, 5.0 and 10.0 $m^{0.8}$). It can be seen that the magnitude of the critical threshold influences the time taken to reach maximum sediment supply; thus low values of the critical threshold promote rapid network growth and establishment of an equilibrium state in <~100 kyr, whereas higher values cause slower network growth and a longer expansion phase of >~300 kyr. However, the overall form of the supply curve through time is similar in all cases and the results presented here are representative of the basic behavior of the model.

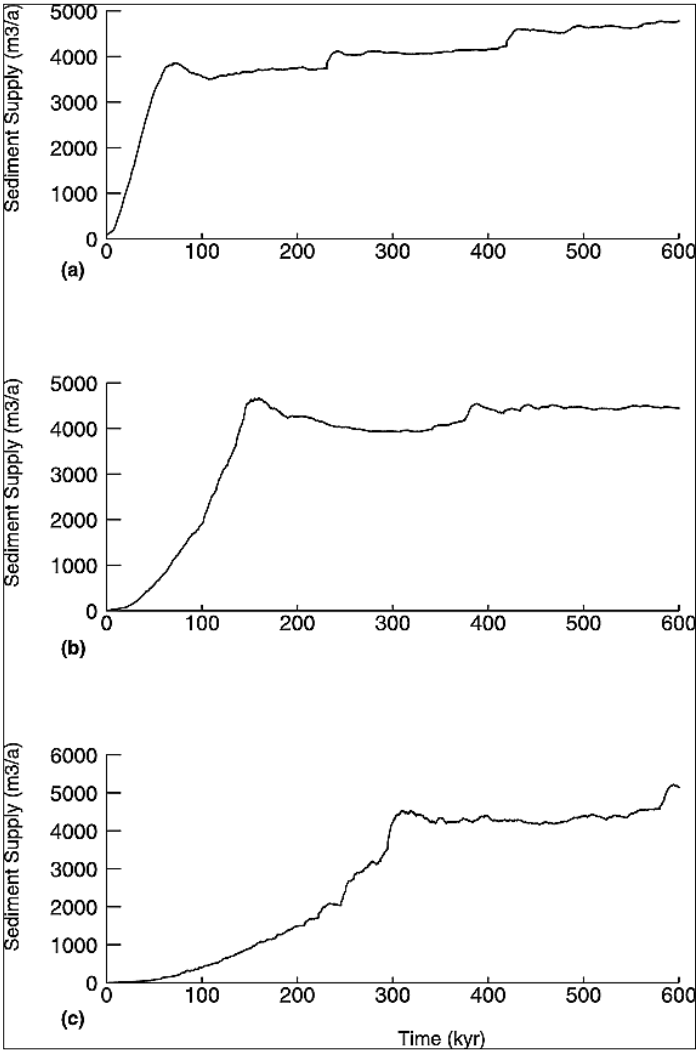


Figure 7. Sediment supply versus time for catchment X indicated in the model shown in Figure 2 in model runs with a range of values of the critical threshold (a) 2.5, (b) 5.0, and (c) 10.0 $m^{0.8}$.

[22] The evolution through time and variability of sediment supply shown by these catchments is representative of the behavior of the model as a whole and arises due to a number of factors. First, the simple growth (expansion) of a stream network in response to repeated footwall uplift events leads to an increasing total stream length with time resulting in many more potential sites for erosion as uplift-related base level perturbations propagate through the system. This leads to an "expansion" phase during which sediment supply to the depositional basin

increases. The transition from isolated to coalesced deltas seen through time in Figure 2 is easily explained in this context, it is the result of the increase in sediment supply as the drainage networks grow through time. As the drainage basin reaches its maximum spatial extent the sediment supply becomes approximately constant as the total channel length is no longer increasing. Thus there is a distinct time lag between the onset of tectonic activity and the attainment of maximum sediment supply from footwall drainage basins. In these examples the time lag is of the order of 125–150 kyr. Second, as the stream networks grow, they alter the flow paths of the distributed injection (rainfall) across the topographic surface. Such changes in flow paths can have a major effect upon the stream power at each site, *Px*, as this depends on both the local gradient and on nonlocal conditions defined by the contributing area at that location. These changes can be minor or extensive depending on the precise configuration of the network when they occur, and can lead to "avalanches" of sediment supply as the critical threshold for erosion is exceeded at a large number of sites. Thus, as the network grows and readjusts it is continually changing both local and global conditions, causing fluvial erosion and leading to variations in sediment supply. With constant tectonic forcing the stream network eventually stabilizes to a fixed configuration after which a steady state is achieved and sediment supply from each catchment is constant.

[23] Figure 8a shows the internal stratigraphy developed in a dip-oriented section through the delta fed by catchment Y indicated in Figure 2. The delta is dominantly aggradational for the first ~25 kyr of the model run with the shoreline trajectory climbing between 40° and vertical. The largely aggradational geometry immediately after the initiation of tectonic activity is due to sediment supply being low compared to the creation of accommodation space due to hanging wall subsidence (Figures 5 and 8a).Stratigraphic architecture then becomes more strongly progradational, with the shoreline climbing at an average angle of 5–10° between 25 and 200 kyr as a result of the increase in sediment supply compared to accommodation space. For the rest of the model run the stacking patterns once again become dominantly aggradational, with the shoreline trajectory increasing to ~30° and then becoming vertical in the last 200 kyr of the model run, as sediment supply becomes approximately constant and the depositional system reaches an equilibrium between sediment supply and accommodation. Some higher-frequency phases of progradation and aggradation can be observed and are related to the variations in sediment supply seen in Figure 5. The stratigraphy developed within the delta clearly reflects the organization of the stream network and thus the inherent variability of sediment supply over both long ($10^5$ years) and short ($10^3$years) timescales. Such variations have typically not previously been considered when modeling the development of coarse-grained deltas. For comparative purposes, Figure 8b shows the internal stratigraphy developed in a delta modeled as having a constant sediment supply of 6500 $m^3$ $yr^{-1}$throughout the 600 kyr of the model run. All other controls are the same as in Figure 8a, and the delta in Figure 8b has essentially the same external morphology. For the first 100 kyr the delta in Figure 8b is strikingly progradational, with the shoreline trajectory climbing at ~10°. Such marked progradation reflects the low accommodation development compared to the time-averaged sediment supply. Continued hanging wall subsidence, combined with increasing water depth and topset length, leads to aggradation between 100 and 250 kyr followed by retrogradation for the rest of the model run. During the retrogradational phase the shoreline climbs in a landward direction at an angle of ~50°. The marked differences in stratal geometry and stacking patterns between the two deltas illustrated in Figure 8 highlights the importance of stream network evolution and the resulting temporal variations in sediment supply as a control on stratigraphic architecture in this structural setting.

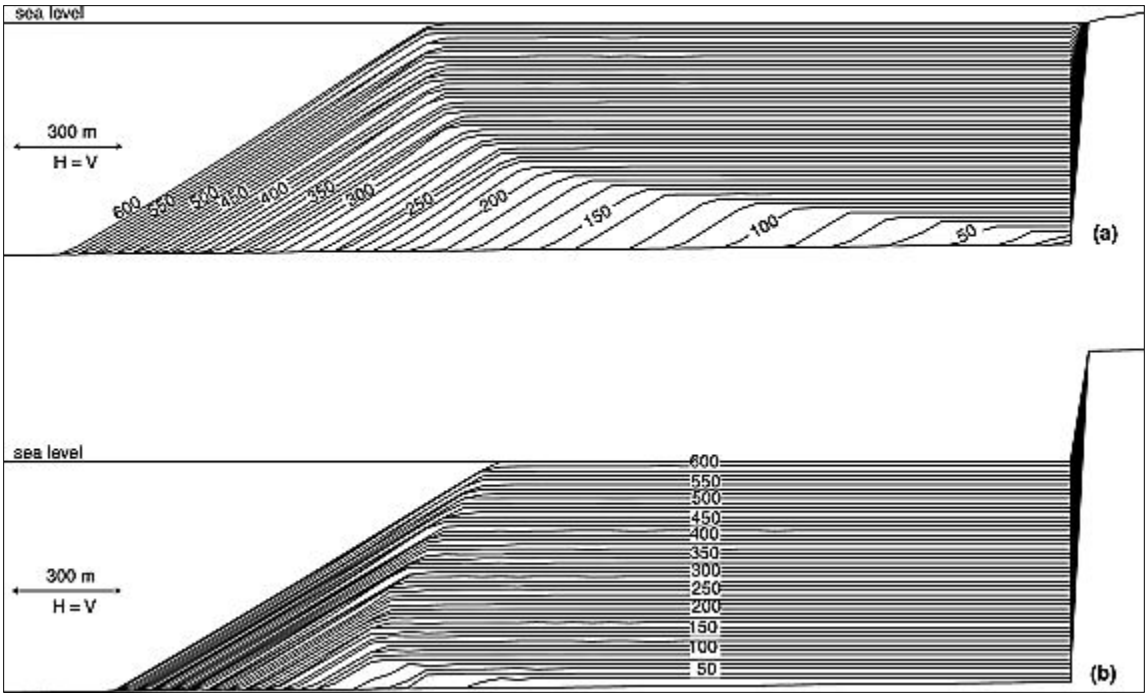


Figure 8. (a) Internal stratigraphy of fan deltas shown in a representative dip-oriented section through the delta fed by catchment Y. (b) Comparative internal stratigraphy of a delta developed under conditions of constant sediment supply. In both cases the stratigraphy is recorded/displayed at intervals of 12.5 kyr and highlighted every 50 kyr. No vertical exaggeration.

### 3.2.2. Changes in Magnitude of Uplift/Subsidence Events

[24] In the model shown above, after the stream networks have reached their maximum spatial extent they reach a steady state where no further topologic adjustments are possible and the network configuration is frozen. With a constant recurrence interval between uplift events this will lead to constant sediment supply from every catchment. Such conditions are unlikely for a variety of reasons, both internal to the system (river avulsion, landslides, etc.) and external (variations in the timing and magnitude of uplift/subsidence events) [see *Hasbargen and Paola*, 2000]. In this section we examine the response of the model to sudden changes in tectonic forcing, in particular, the magnitude of the paired uplift/subsidence events. The experiments will show the response of the model to faulting events that happen (as before) every 1000 years but whose magnitude changes abruptly halfway through the model run (300 kyr). For the first 300 kyr of the model run these events cause the hanging wall to subside by 1.0 m and the footwall to uplift by 0.5 m. In the first experiment (Figures 9a and 10a) the magnitude of uplift/subsidence events halves from that experienced in the first 300 kyr of the model run to 0.25 m of uplift paired with 0.50 m of subsidence. In the second experiment (Figures 9b and 10b) the magnitude of uplift/subsidence events doubles from that experienced in the first 300 kyr of the model run to 1.0 m of uplift and 2.0 m of subsidence. All other model parameters are identical to those used in the previous model.

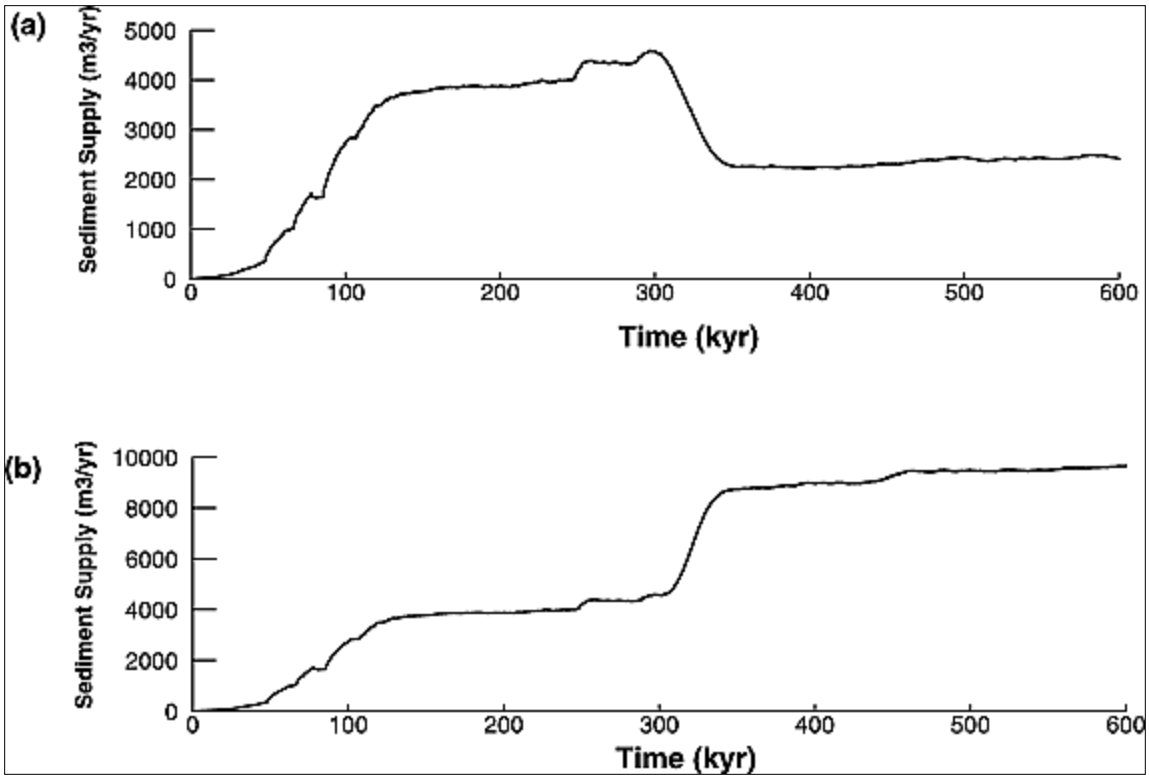


Figure 9. Sediment supply versus time for the catchment Y under conditions of (a) an instantaneous 50% decrease in the magnitude of uplift/subsidence events at 300 kyr and (b) an instantaneous 200% increase in the magnitude of uplift/subsidence events at 300 kyr.

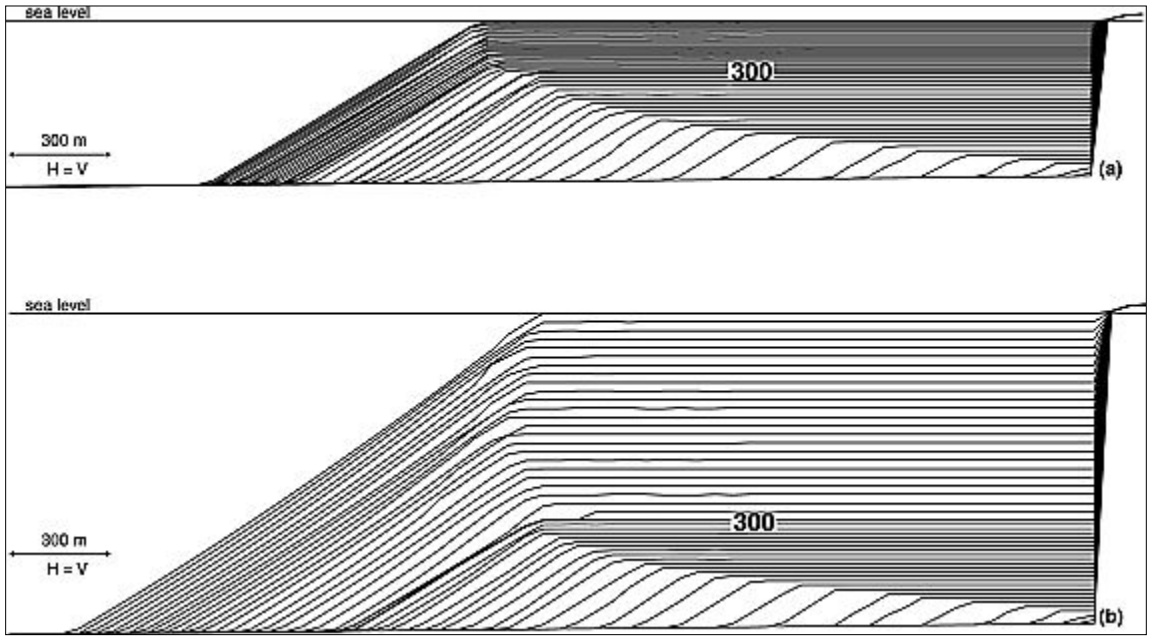


Figure 10.Internal stratigraphy of fan deltas shown in a representative dip-oriented section through the delta fed by catchment Y for conditions shown in Figures 9a and 9b. In both cases the stratigraphy is recorded/displayed at intervals of 12.5 kyr and highlighted every 50 kyr. No vertical exaggeration.

[25] The response of the model to a sudden decrease in the magnitude of the uplift/subsidence events is illustrated with respect to catchment Y discussed above and illustrated in Figure 2. Figure 9a shows the sediment supply from this catchment throughout the model run. The decrease in both uplift and subsidence by 50% at 300 kyr has a dramatic effect; sediment supply decreases from ~4200 to ~2300 $m^3yr^{-1}$ as the system responds to the change and attains a new steady state. However, the new steady state is not achieved instantaneously; rather it takes place over a period of ~50 kyr. The change in sediment supply and accommodation is very clearly expressed in the stratigraphy of the deltaic deposits fed by catchment Y (Figure 10a). Initially, the decrease in uplift/subsidence produces a progradational geometry in the delta as the sediment supply has not yet adjusted to (lags behind) the new uplift rate while the rate of accommodation creation has halved. Thus the sediment supply is greater than accommodation creation and the delta progrades. However, within 50 kyr the delta becomes strikingly aggradational as the sediment supply reaches its new, lower steady state value and reaches equilibrium with the creation of accommodation space.

[26] The case of a sudden increase in the magnitude of uplift/subsidence events is also illustrated with respect to catchment Y. Figure 9b shows the sediment supply from this catchment throughout the model run. The increase in both uplift and subsidence by a factor of two at 300 kyr has a dramatic effect; sediment supply increases from ~4200 to ~9500 $m^3\ yr^{-1}$ as the system responds to the change and attains a new steady state. However, as before, the new steady state is not achieved instantaneously, rather it takes place over a period of ~50 kyr. This change in sediment supply and accommodation is very clearly expressed in the stratigraphy of the deltaic deposits fed by catchment Y (Figure 10b). Initially, the increase in uplift/subsidence produces a retrogradational geometry in the delta as the sediment supply has not yet adjusted to the new uplift rate and the rate of accommodation creation has doubled. However, the delta then becomes progradational and then strikingly a gradational as the sediment supply reaches it's new, higher steady state value.

### 3.2.3. Variable Recurrence Interval

[27] The final experiment will show the response of the model to repeated faulting events that happen on average every 1000 years but whose timing is variable leading to random clustering and quiescence of tectonic activity throughout the 600 kyr of the model run. As before, these events cause the hanging wall to subside by 1.0 m and the footwall to uplift by 0.5 m, but the recurrence interval between events varies between 100 and 1900 years. All other model parameters are identical to those used in the previous model. Figure 11 shows the response of catchment Y in terms of sediment supply (Figure 11a) to the variation in recurrence interval (Figure 11b). It can be seen that while the overall form of the sediment supply curve is similar to the previous models it exhibits much more variation. In particular, it does not reach a steady state but rather shows major pseudocyclic variations in sediment supply of ~1000 $m^3\ yr^{-1}$(~20% of the steady state value) in response to periods of increased and decreased tectonic activity. Figure 12 shows the stratigraphic architectures developed in response to this sediment supply. Overall the stratigraphic architecture is similar to previous models but shows phases of aggradation, progradation, and retro gradation in response to the high-frequency changes in sediment supply shown in Figure 11a. It is interesting to note that while the variations in sediment supply in response to tectonic activity are striking, their expression in the stratigraphic record is less so. It appears that the overall form of the sediment supply curve through time dictates the basic form of the delta, whereas the higher-frequency variations result in shifts in shoreline position but not necessarily major architectural differences.

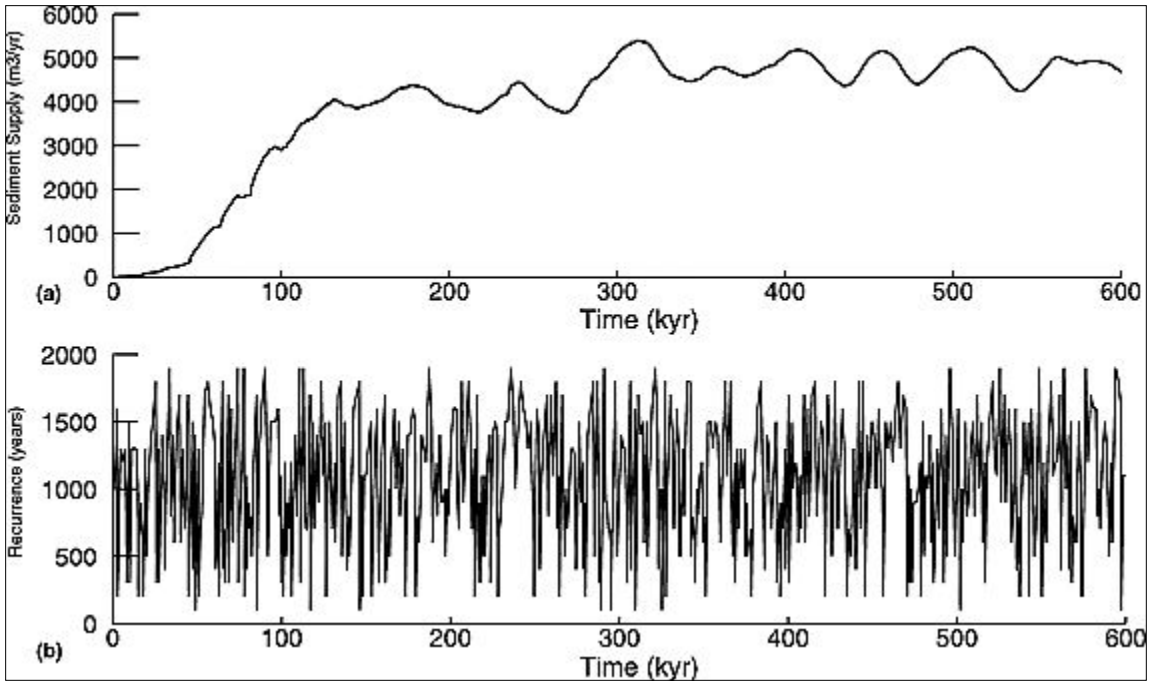


Figure 11.(a) Sediment supply versus time for the catchment Y under conditions variable recurrence interval between uplift events. (b) Variation in recurrence interval through model run.

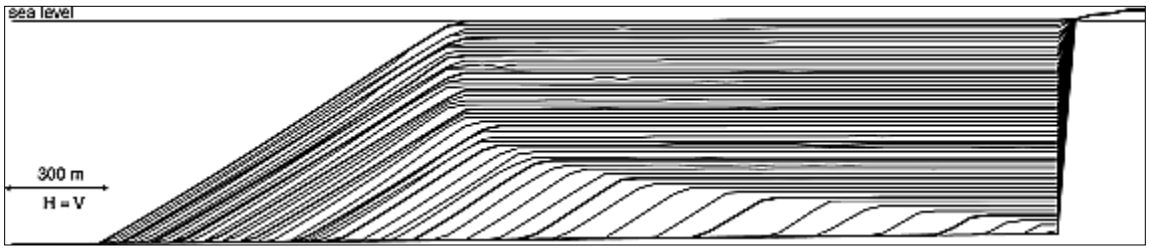


Figure 12. Internal stratigraphy of fan deltas shown in a representative dip-oriented section through the delta fed by catchment Y for conditions shown in Figure 11. The stratigraphy is recorded/displayed at intervals of 12.5 kyr and highlighted every 50 kyr. No vertical exaggeration.

## 4. Discussion

### 4.1. Variability of Sediment Supply From Bedrock Channel Dominated Catchments

[28] The small, mountainous catchments considered here are the source of many coarse-grained alluvial fans and fan deltas, the focus of much recent stratigraphic research as they have the potential for recording tectonic, climatic, and eustatic variations in their preserved stratigraphy [e.g., *Colella*, 1988; *Gawthorpe and Colella*, 1990; *Dart et al.*, 1994; *Dorsey et al.*, 1995, 1997]. Sequence stratigraphic models are commonly applied to interpret the controls on such deltas and generally neglect temporal variations in sediment supply. Stratal relationships and facies distributions are instead interpreted largely as a function of regional variations in the rate of relative sea level change or at best variations in the accommodation/sediment supply ratio. However, it is now recognized that drainage basin response to climatic and tectonic forcing and the resultant variations in sediment supply can have major effects upon the spatial and temporal

variability of depositional sequences in sedimentary basins [e.g., *Leeder*, 1991; *Hardy et al.*, 1994; *Eliet and Gawthorpe*, 1995].

[29] The coupled LEM-deltaic deposition model presented here provides insights into the first-order variations in sediment supply from bedrock channel dominated catchments due to tectonic forcing, and confirms the view that variations in sediment supply are an important control on sequence architectures in small, coarse-grained fan deltas. Much of this variability in sediment supply is related to the dynamics of stream network growth and organization and is not necessarily directly related to specific tectonic (coseismic) events. Experimental results indicate that the evolution and organization of bedrock channel networks in response to repeated footwall uplift events (coseismic slip) leads to a progressively increasing sediment supply over a period of many tens of thousands of years as the networks expand. This is followed by a period of approximately constant sediment supply as the stream networks reach their maximum spatial extent. There is a significant time lag (~100–125 kyr for the model parameters used here) between the onset of tectonic activity and the attainment of maximum sediment supply from the drainage basins. However, even within periods of approximate equilibrium, there are fluctuations in sediment supply that are not directly related to, or in phase with, individual faulting (uplift) events. These variations are the product of the complex response and reorganization of the stream networks to faulting-related perturbations and their occurrence is not predictable. With a constant recurrence interval between uplift events the stream networks eventually stabilize to a fixed configuration after which a steady state is achieved and sediment supply from each catchment is constant. When the model is not subject to constant tectonic forcing, through variation in recurrence interval, a true steady state configuration is not reached and much variation in sediment supply, on the order of 1000 $m^3\ yr^{-1}$, is present even when the stream network has reached its maximum spatial extent.

[30] The evolution of channel networks described in this contribution and associated variations in sediment supply have important implications for the interpretation of stratigraphic architectures preserved within sedimentary basin fills. Because of the time lag between initiation of tectonic activity and maximum sediment supply, stacking patterns in the modeled fan deltas are initially aggradational but then become progradational. Changes in shoreline trajectory and in the amount of progradation shown in the stratigraphic architectures of the modeled fan deltas can be related to higher frequency variations in sediment supply. These stacking patterns are unrelated to any specific changes in tectonic activity. Great caution must therefore be taken when examining preserved stratigraphic architectures and ascribing stacking patterns to specific external factors. When the model is subjected to changes in recurrence interval between events the response is complex: large variations in sediment supply are produced but it appears that much of the large-scale stratigraphic architecture of the fan deltas is a reflection of stream network growth. The modeled variations in sediment supply are expressed over geologically short timescales ($10^3$–$10^4$ years) that are extremely difficult to resolve using current radiometric or biostratigraphic data especially within coarse-grained deltaic deposits. Nevertheless, such intrinsic variations must be borne in mind when examining and interpreting the (typically) poorly temporally calibrated stratigraphic architectures seen in many ancient fan deltas. The (sequence) stratigraphic interpretation of such stratigraphic architectures must be therefore done with caution.

### 4.2. Assumptions and Improvements

[31] We have chosen to examine a system in which fluvial erosion and uplift are the dominant processes contributing to sediment supply to adjacent sedimentary basins. In doing so,

we are simplifying a very complex system by making several assumptions and restrictions that may limit the model's general applicability.

[32] First, the model is strictly only applicable to small, mountainous catchments such as those that are commonly found in tectonically active regions and where bedrock channels can be expected to be the dominant channel type [*Tucker and Slingerland*, 1996]. The model is not appropriate for transport-limited fluvial systems that are an important component of many larger catchments [e.g., *Howard et al.*, 1994].

[33] Second, we do not include processes such as hillslope diffusive transport or landsliding in our model [cf. *Rigon et al.*, 1994; *Densmore et al.*, 1998]. These are clearly important processes which contribute to the sediment supply to the depositional basin, but we have chosen to focus on a bedrock channel LEM in order to isolate sediment supply variations due solely to the response of the fluvial network to imposed tectonic perturbations. We have taken this approach as in many tectonically active regions; it can be argued that topographic evolution is dominated by the rates and patterns of bedrock channel incision [*Snyder et al.*, 2000]. Bedrock incision appears to be the rate limiting process in many landscapes, influencing gradients on adjacent hillslopes and being closely coupled with land sliding [*Densmore et al.*, 1998]. Clearly, the inclusion of hillslope diffusive transport and landsliding in our model would affect the equilibrium state of our model; however, the products of these processes must find their way into bedrock channels and be acted upon by stream channel discharges. Thus our predicted sediment supplies can be thought of as first-order sediment supplies that will clearly be modulated and altered by contributions from landsliding and hillslope transport.

[34] Third, the model of detachment-limited, bedrock channel evolution used here is only one of many [see *Veneziano and Niemann*, 2000a]. We have chosen to use a stream power incision law due to its simplicity and ability to capture the behavior of many river networks and to reproduce the fractal characteristics of real landscapes. Our choice of the exponents $m$ and $n$ in the stream power erosion law limits the scope of our analysis, but a fuller investigation of the effects of different exponent values (e.g., $m = 1/3$, $n = 2/3$, erosion rate linearly proportional to shear stress) is underway.

[35] Finally, we are using a very simple structural “template” to produce the tectonic uplift forcing the evolution of the bedrock channels. In reality, natural structures exhibit significant along-strike variation in uplift along fault segments, flexural uplift in the footwall, and both horizontal and vertical components of motion in the displacement field [e.g., *Leeder and Jackson*, 1993]. These factors will have an effect upon uplift both spatially and temporally and are the subject of ongoing research.

[36] While we have considered here the influence of tectonics on stream network development and sediment supply, climate can clearly also modulate the response of this complex system through both changes in precipitation (surface water flow), vegetative cover and local or regional base level [e.g., *Rinaldo et al.*, 1995; *Whipple et al.*, 1999]. Such effects are clearly of great importance and are the focus of ongoing research.

## 5. Conclusions

[37] This paper has investigated, through numerical modeling, the evolution of stream (bedrock channel) networks in the footwalls of extensional fault blocks, the spatial and temporal evolution of sediment supply to hanging wall basins, and the resultant stratigraphic architectures in fan deltas. The numerical model presented and used here is a simplification of a very complex

system, but we feel that it allows us to make the following statements regarding the evolution of sediment supply from bedrock channel dominated drainage basins:

1. The evolution and organization of bedrock channel networks in response to repeated footwall uplift events leads to a progressively increasing sediment supply over a period of many tens of thousands of years as the networks initiate and then expand. This is followed by a period of relatively constant sediment supply, as the stream networks reach their maximum spatial extent. Thus there is a distinct time lag between the onset of tectonic activity and the attainment of maximum sediment supply from footwall drainage basins. However, even within this period of approximate equilibrium there are fluctuations in sediment supply that are not in phase with specific faulting (uplift) events. These variations are the product of the complex response and reorganization of the stream networks to faulting-related perturbations and their occurrence is not predictable. With a constant recurrence interval between uplift events the stream network eventually stabilizes to a fixed configuration after which a steady state is achieved and sediment supply from each catchment is constant.

2. These variations, both systematic and random, can have a significant effect upon the stratigraphic architecture of fan deltas fed by such drainage basins. Because of the increasing sediment supply with time, stacking patterns in the modeled fan deltas are initially aggradational but then become strongly progradational. Individual phases of progradation and aggradation can be related to higher-frequency variations in sediment supply. Such intrinsic variations must be borne in mind when examining and interpreting the (typically) uncelebrated stratigraphic architectures seen in many ancient fan deltas.

3. When the model is not subject to constant tectonic forcing, through variation in recurrence interval, a true steady state configuration is not reached and much inherent variation in sediment supply is present even when the stream networks have reached their maximum spatial extent.

## Reference


Bak, P., C. Tang, and K. Wiesenfeld, Self-organised criticality, *Phys. Rev. A,* 38(1), 364—374, 1988.

Caldarelli, G., A. Giacometti, A. Maritan, I. Rodriguez-Iturbe, and A. Ri-naldo, Randomly pinned landscape evolution, *Phys. Rev. E,* 55(5), R4865—R4868, 1997.

Colella, A., Pliocene-Holocene fan deltas of the Messina Strait, in *Fan Deltas—Excursion Guidebook,* edited by A. Colella, pp. 139 — 152, Univ. della Calabria, Consenza, Italy, 1988.

Dart, C. J., R. E. L. Collier, R. L. Gawthorpe, J. V. Keller, and G. Nichols, Sequence stratigraphy of (?) Pliocene-Quaternary syn-rift, Gilbert-type deltas, northern Peloponnesos, Greece, *Mar. Pet. Geol., 11*, 545 — 560,1994.

Densmore, A., M. A. Ellis, and R. S. Anderson, Landsliding and the evolution of normal-fault-bounded mountains, *J. Geophys. Res., 103,* 15,203 — 15,220, 1998.

Dorsey, R. J., P. J. Umhoefer, and P. R. Renne, Rapid subsidence and stacked Gilbert-type fan deltas, Pliocene Loreto basin, Baja CaliforniaSur, Mexico, *Sediment. Geol, 98,* 181—204, 1995.

Dorsey, R. J., P. J. Umhoefer, and P. D. Falk, Earthquake clustering inferred from Pliocene Gilbert-type deltas in the Loreto basin, Baja California Sur,Mexico, *Geology, 25,* 679—682, 1997.

Driscoll, N. W., and G. D. Karner, Three-dimensional quantitative modeling of clinoform development, *Mar. Geol., 154,* 383—398, 1999.

Eliet, P. P., and R. L. Gawthorpe, Drainage development and sediment supply within rifts, examples from the Sperchios basin, central Greece, *J. Geol. Soc. London, 152,* 883 — 893, 1995.

Gawthorpe, R. L., and A. Colella, Tectonic controls on coarse-grained depositional systems in rift basins, in *Coarse-Grained Deltas,* edited by A. Colella and D. B. Prior, *Spec. Publ. Int. Assoc. Sedime ntol.,* 10,113 —127, 1990.

Gawthorpe, R. L., A. J. Fraser, and R. E. L. Collier, Sequence stratigraphy in active extensional basins:

Implications for the interpretation of ancient basin fills, *Mar Pet. Geol., 11,* 642—658, 1994.
Goldsworthy, M., and J. Jackson, Active normal fault evolution in Greece revealed by geomorphology and drainage patterns, *J. Geol. Soc. London,157,* 967—981, 2000.
Hardy, S., and R. L. Gawthorpe, Effects of variations in fault slip rate on sequence stratigraphy in fan deltas: Insights from numerical modeling, *Geology, 26,* 911—914, 1998.
Hardy, S., C. Dart, and D. Waltham, Computer modelling of the influence of tectonics upon sequence architecture of coarse-grained fan deltas, *Mar.Pet. Geol., 11*, 561—574, 1994.
Hasbargen, L. E., and C. Paola, Landscape instability in an experimental drainage basin, *Geology, 28,* 1067 — 1070, 2000.
Howard, A. D., A detachment-limited model of drainage basin evolution, *Water Resour. Res., 30,* 2261—2285, 1994.
Howard, A. D., W. E. Dietrich, and M. A. Siedl, Modeling fluvial erosion on regional to continental scales, *J. Geophys. Res., 99,* 13,971 — 13, 986, 1994.
Leeder, M. R., Denudation, vertical crustal movements and sedimentary basin fill, *Geol. Rundsch, 80,* 441—458, 1991.
Leeder, M. R., and J. A. Jackson, The interaction between normal faulting and drainage in active extensional basins, with examples from the western United States and central Greece, *Basin Res., 5,* 79 — 102, 1993.
Nemec, W., Aspects of sediment movement on steep delta slopes, in *Coarse-Grained Deltas,* edited by A. Colella and D. B. Prior, *Spec. PublInt. Assoc. Sedimentol., 10,* 29—73, 1990.
Pelletier, J. D., Self-organization and scaling relationships of evolving river networks, *J. Geophys. Res., 104,* 7359—7375, 1999.
Rigon, R., A. Rinaldo, and I. Rodriguez-Iturbe, On landscape self-organisation, *J. Geophys. Res., 99,* 11,971 — 11,985, 1994.
Rinaldo, A., W. E. Dietrich, R. Rigon, G. K. Vogel, and I. Rodriguez-Iturbe, Geomorphological signatures ofvarying climate, *Nature, 374,* 632—635,1995.
Ritchie, B., S. Hardy, and R. Gawthorpe, Three-dimensional modelling of coarse-grained clastic deposition in sedimentary basins, *J. Geophys. Res.,* 104, 17,759 — 17,780, 1999.
Rodriguez-Iturbe, I., and A. Rinaldo, *Fractal River Basins, Chance and Self-Organization,* 547 pp., Cambridge Univ. Press, New York, 1997.
Snyder, N. P., K. X. Whipple, G. E. Tucker, and D. J. Merritts, Landscape response to tectonic forcing: digital elevation model analysis of stream profiles in the Mendocino triple junction region, northern California,*Geol. Soc. Am. Bull., 112,* 1250—1263, 2000.
Stark, C. P., An invasion percolation model ofdrainage networkevolution,*Nature, 352,* 423—425, 1991.
Stock, J. D., and D. R. Montgomery, Geologic constraints on bedrock river incision using the stream power law, *J. Geophys. Res., 104,* 4983-4993,1999.
Talling, P. J., Self-organization of river networks to threshold states, *Water Resour. Res., 36,* 1119-1128, 2000.
Tinkler, K., and E. Wohl, A primer on bedrock channels, in *Rivers Over Rock - Fluvial Processes in Bedrock Channels, Geophys. Monogr. Ser.*, vol. 107, edited by K. Tinkler and E. E. Wohl, pp. 1-18, AGU, Washington, D. C., 1998.
Tucker, G. E., and R. Slingerland, Predicting sediment flux from fold and thrust belts, *Basin Res., 8,* 329-349, 1996.
Tucker, G. E., and R. Slingerland, Drainage basin responses to climate change, *Water Resour. Res., 33, ]* 2031-2047, 1997.
Van der Beek, P., and J. Braun, Controls on post-mid-Cretaceous landscape evolutionin the southeastern highlands ofAustralia:Insights fromnumer-ical surface process models, *J. Geophys. Res., 104,* 4945-4966, 1999.
Veneziano, D., and J. D. Niemann, Self-similarity and multifractality of fluvial erosion topography, 1, Mathematical conditions and physical origin, *Water Resour. Res., 36,* 1923-1936, 2000a.
Veneziano, D., and J. D. Niemann, Self-similarity and multifractality of fluvial erosion topography, 2, Scaling properties, *Water Resour. Res.* , 36, 1937-1951, 2000b.
Whipple, K. X., and G. E. Tucker, Dynamics of the stream-power river incision model: Implications for height limits of mountain ranges, landscape response timescales, and research needs, *J. Geophys. Res., 104,*17,661 -17,674, 1999.
Whipple, K. X., E. Kirby, and S. H. Brocklehurst, Geomorphic limits to climate-induced increases in \

topographic relief, *Nature, 401*,39-43,1999.
Whipple, K. X., N. P. Snyder, and K. Dollenmayer, Rates and processes of bedrock incision by the Upper Ukak River since the 1912 Novarupta ash flow in the Valley of Ten Thousand Smokes, Alaska, *Geology, 28,* 835838, 2000a.
Whipple, K. X., G. S. Hancock, and R. S. Anderson, River incision into bedrock: Mechanics and relative efficacy of plucking, abrasion, and ca-vitation, *Geol. Soc. Am. Bull., 112,* 490-503, 2000b.
Young, M. J., R. L. Gawthorpe, and I. R. Sharp, Sedimentology and sequence stratigraphy of a transfer zone coarse-grained delta: Miocene Suez rift, Egypt, *Sedimentology, 47,* 1081-1104, 2000.